Biochemistry and Biophysics Reports 24 (2020) 100868

Contents lists available at ScienceDirect

Biochemistry and Biophysics Reports

journal homepage: www.elsevier.com/locate/bbrep

RELT stains prominently in B-cell lymphomas and binds the hematopoietic transcription factor MDFIC

John K. Cusick [a,*], Yasmeen Alhomsy [a], Stephanie Wong [b], George Talbott [c], Vladimir N. Uversky [d], Cara Hart [e], Nazila Hejazi [f], Aaron T. Jacobs [b], Yihui Shi [a]

[a] Department of Basic Science, California Northstate University, College of Medicine, Elk Grove, CA, 95757, USA
[b] Department of Medical Education, California University of Science and Medicine, San Bernardino, CA, 92408, USA
[c] Department of Pharmaceutical and Biomedical Sciences, California Northstate University College of Pharmacy, Elk Grove, CA, 95757, USA
[d] Department of Molecular Medicine and USF Health Byrd Alzheimer's Research Institute, Morsani College of Medicine, University of South Florida, Tampa, FL, 33612, USA
[e] Department of Biology, The University of Hawaii at Hilo, Hilo, HI, 96720, USA
[f] Department of Clinical Science, California Northstate University, College of Medicine, Elk Grove, CA, 95757, USA

ARTICLE INFO

Keywords:
RELT
RELL1
RELL2
TNFRSF
MDFIC
B-Cell lymphoma
Disordered proteins

ABSTRACT

Receptor Expressed in Lymphoid Tissues (RELT) is a human tumor necrosis factor receptor superfamily member (TNFRSF) that is expressed most prominently in cells and tissues of the hematopoietic system. RELL1 and RELL2 are two homologs that physically interact with RELT and co-localize with RELT at the plasma membrane. This study sought to further elucidate the function of RELT by identifying novel protein interactions with RELT family members. The transcription factor MyoD family inhibitor domain-containing (MDFIC) was identified in a yeast two-hybrid genetic screen using RELL1 as bait. MDFIC co-localizes with RELT family members at the plasma membrane; this co-localization was most prominently observed with RELL1 and RELL2. In vitro co-immunoprecipitation (Co-IP) was utilized to demonstrate that MDFIC physically interacts with RELT, RELL1, and RELL2. Co-IP using deletion mutants of MDFIC and RELT identified regions important for physical association between MDFIC and RELT family members and a computational analysis revealed that RELT family members are highly disordered proteins. Immunohistochemistry of normal human lymph nodes revealed RELT staining that was most prominent in macrophages. Interestingly, the level of RELT staining significantly increased progressively in low and high-grade B-cell lymphomas versus normal lymph nodes. RELT co-staining with CD20 was observed in B-cell lymphomas, indicating that RELT is expressed in malignant B cells. Collectively, these results further our understanding of RELT-associated signaling pathways, the protein structure of RELT family members, and provide preliminary evidence indicating an association of RELT with B-cell lymphomas.

1. Introduction

Tumor necrosis factor receptor superfamily (TNFRSF) members are transmembrane proteins critical for the regulation of many biological processes including cell death, inflammation, cellular differentiation, and development [1,2]. Many therapeutic agents designed to modulate TNFRSF signaling are utilized for the treatment of a variety of diseases including inflammation, autoimmunity, and cancer [3]. TNFRSF members initiate signaling responses that alter cellular behavior, typically in response to binding by trimeric tumor necrosis factor superfamily (TNFSF) member ligands, which can be either soluble or attached to another cell. There are currently 19 distinct TNFSF ligands and 29 TNFRSF members identified in humans [1].

Receptor expressed in lymphoid tissues (RELT) is a TNFRSF member (TNFRSF19L) that is expressed predominantly in the hematopoietic system [4–6]. RELT is an orphan receptor as the ligand for RELT has not been identified. RELL1 and RELL2 (RELT Like 1 and 2 respectively) are two RELT paralogs that are considered RELT family members, as they both physically bind RELT and co-localize with RELT at the plasma membrane [7]. Overexpression of RELT family members induces apoptosis in human epithelial cells with characteristics consistent of an apoptotic pathway [8]. RELT family members activate the p38 MAPK

* Corresponding author. California Northstate University College of Medicine, Elk Grove, CA, USA.
E-mail address: john.cusick@cnsu.edu (J.K. Cusick).

https://doi.org/10.1016/j.bbrep.2020.100868
Received 28 July 2020; Received in revised form 2 November 2020; Accepted 23 November 2020

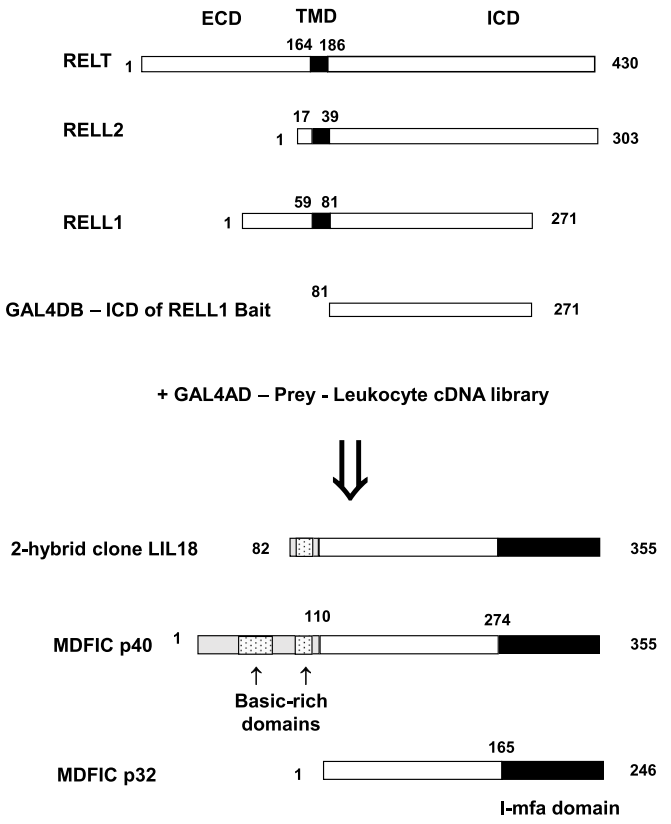

Fig. 1. MDFIC identified in a two-hybrid screen utilizing RELL1 as bait. Schematic showing the RELT family members, the two isoforms of MDFIC, and the LIL18 clone obtained in the two-hybrid screen. The transmembrane domains of RELT family members are highlighted in black. The intracellular domain of RELL1 was utilized as bait in a two-hybrid screen as described in Materials and Methods. LIL18 encodes a truncated fragment of the p40 isoform of MDFIC expressed in-frame with the GADD activation domain. Relative sizes of the two forms of MDFIC, p32, and p40, are shown. The carboxy-terminal I-mfa domain of MDFIC is shown in black, and the basic-rich regions implicated in nuclear and nucleolar import of p40 are highlighted. LIL18 clone contains sequences encoding the entire p32 region in addition to 28 amino acids of sequences exclusive to p40, including one of the two basic-rich domains.

pathway in a manner that requires phosphorylation by the closely related kinases OSR1 and SPAK [5,9]. Mice lacking RELT exhibit increased proliferation of $CD4^+$ T helper cells and increased anti-tumor responses by $CD8^+$ T cells, collectively indicating that RELT functions in part as a negative regulator of T cell responses [6]. Non-biased searches identified an upregulation of serum RELT in gastric cancer [10] and autoantibodies directed against RELT in breast cancer [11]. Furthermore, RELT is upregulated in lung cancer and was identified as the receptor for peptide-mediated liposome delivery of therapeutics to cancerous lung tissue in mice [12]. Cleavage of the RELT extracellular domain (ECD) is required for enamel development [13] and mutations in the *RELT* gene are associated with amelogenesis imperfecta [14,15].

Although RELL1 and RELL2 have been proposed to modulate signaling by RELT [7] based on the lack a cysteine-rich ECD characteristic of other TNFRSF members (Fig. 1), recent reports indicate that RELL1 and RELL2 possess functions independent of RELT. RELL1 influences infectious processes, as it enhances *M. tuberculosis* survival in macrophages by inhibiting autophagy [16] and a downregulation of RELL1 is associated with HCMV latency [17]. RELL1 has been proposed to serve as an oncogene, as it is upregulated and associated with poor prognosis in gliomas [18]. Conversely, RELL2 possesses anti-tumor activity, as RELL2 expression inhibits migration and invasion of breast cancer cells [19], and inhibits the tumorigenic potential of esophageal cancer cells [20]. The *RELL1* and *RELL2* mRNA transcripts appear to have functions independent of the translated protein, as a circular RNA molecule transcribed from the *RELL1* gene is pro-inflammatory in endothelial cells and may contribute to cardiovascular disease [21], while a long non-coding RNA transcribed from the *RELL2* gene is associated with better prognosis for patients with intrahepatic cholangiocarcinoma [22].

In this study, a yeast two-hybrid genetic screen was conducted utilizing the intracellular domain of RELL1 as bait to identify MyoD Family Inhibitor Domain Containing (MDFIC), also known as HIC (Human I-mfa Domain containing protein) [23], as a novel protein that binds RELT family members. We describe the co-localization of MDFIC with RELT family members in human embryonic kidney 293 (293) cells and the regions of MDFIC and RELT required for this physical association. Regions of RELT that bind MDFIC did not contain conserved structural motifs and further computational analysis of protein structure revealed that RELT family members are intrinsically disordered proteins. Finally, to obtain a better understanding of the physiological significance of RELT, we examined the expression of RELT in healthy versus diseased tissues and report preliminary evidence indicating that RELT expression is upregulated in B-cell lymphomas.

2. Materials and Methods

Reagents. The human embryonic kidney 293 (293) cell line was purchased from ATCC. The intracellular portion of RELL1 was cloned into the Gal4 DNA-binding domain vector pGBT9 (Clontech, Palo Alto, CA) as described previously [7]. The expression plasmid constructs for RELT, RELL1, OSR1 [7], and the RELT deletion mutants [5] were described previously. The Flag-tagged RELL2 construct [7] was cloned into the pCMV-HA-C plasmid (Clontech) to create the C-terminal HA-tagged RELL2 expression plasmid described in this report. Expression constructs for full-length and mutant forms of MDFIC were a kind gift from V. Gautier from the University of Dublin. Lipofectamine transfection reagent, the TNFRSF19L antibody used in IHC (PA5-21563), goat polyclonal CD20 antibody (PA1-9024), mouse anti-Flag antibody used for the RELL2-MDFIC Co-IP, and the donkey anti-goat antibody used in immunofluorescence (IF) assays were purchased from ThermoFisher Scientific (Waltham, MA). The Protein G Immunoprecipitation kit (IP50-1 KT) and a mouse anti-HA antibody utilized for western blotting were purchased from Sigma-Aldrich (St. Louis, MO). The polyclonal RELT antibody used to detect RELT deletion mutants (AF1385) was purchased from R&D Systems (Minneapolis, MN). A rabbit polyclonal RELT antibody (ab96220) from Abcam (Burlingame, CA) was used for RELT-CD20 co-localization. Additional antibodies used in Co-IP and IF experiments included the mouse and rabbit anti-DYKDDDDK (equivalent to Flag) tags, rabbit anti-HA tag, Alexa Fluor goat anti-rabbit IgG 555 and goat anti-mouse IgG 488 antibodies, and rabbit IgG control antibodies, purchased from Cell Signaling Technology Inc. (Danvers, MA). The mouse IgG control was purchased from SantaCruz Biotechnologies Inc. (Santa Cruz, CA). IR-800 and IR-680 secondary antibodies used for western blotting were purchased from LI-COR Biosciences (Lincoln, NE). Vectashield mounting medium with DAPI and most IHC reagents other than antibodies were purchased from Vector Laboratories (Burlingame, CA). De-identified unstained sections from normal adult lymph nodes and B-cell lymphomas were obtained from the University of California, Davis Comprehensive Cancer Center (Sacramento, CA).

Immunofluorescence (IF) staining. For MDFIC staining, IF was used as previously described [24] using Lipofectamine as the transfection reagent. 1:1000 dilutions of a mouse anti-Flag and rabbit anti-HA antibody were utilized as primary antibodies. For secondary antibodies, 1:1000 dilutions of the Alexa Fluor goat anti-mouse IgG 488 and Alexa Fluor goat anti-rabbit IgG 555 were utilized. For IF staining of lymph nodes and B-cell lymphomas, fixed tissue sections were incubated with 1:250 and 1:100 dilutions of rabbit anti-RELT and goat anti-CD20 antibodies respectively as primary antibodies, with 1:1000 dilutions of the Alexa

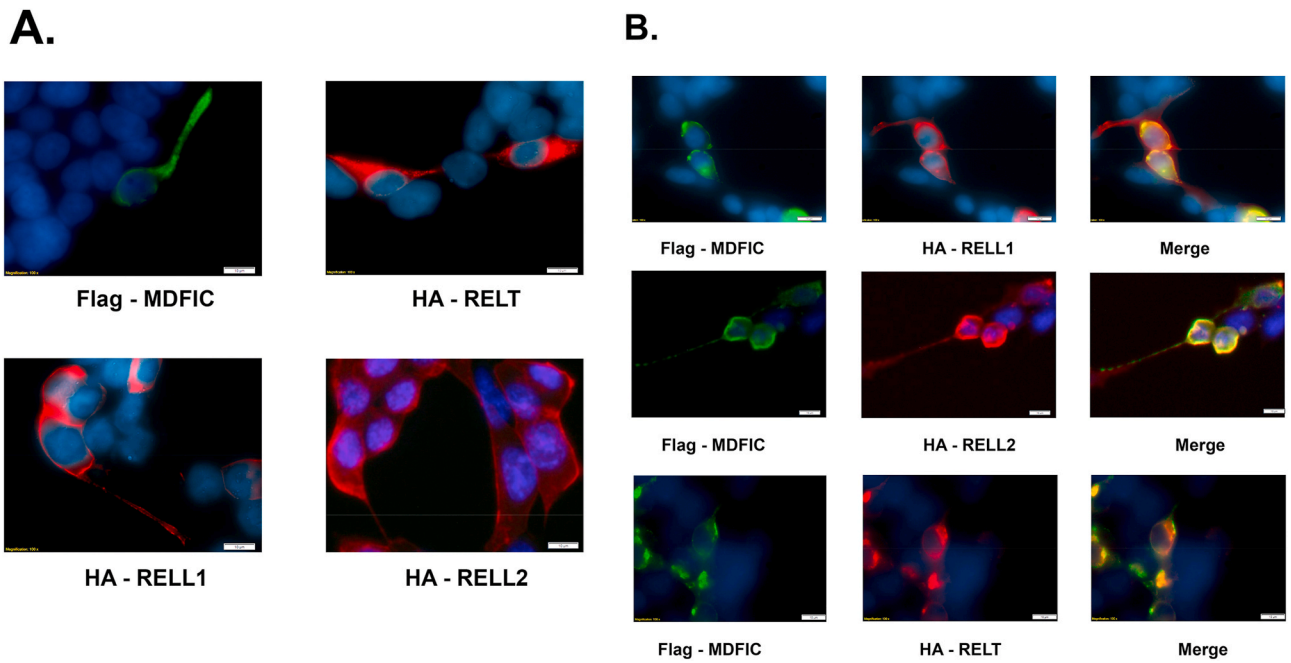

Fig. 2. Co-localization of MDFIC and RELT family members. 293 cells were transiently transfected with the indicated mammalian expression plasmids, followed by fixing the next day for immunofluorescence as described in Materials and Methods. Anti-HA and anti-Flag primary antibodies were used as indicated in combination with Alexa Fluor dye secondary antibodies to detect the presence of the epitope-tagged proteins. This procedure resulted in HA-tagged RELT family proteins fluorescing red and the Flag-tagged p32 isoform of MDFIC fluorescing green. Cells were treated with DAPI to stain DNA blue. Photographs were taken at 40x magnification. (A) Localization of MDFIC and RELT family member proteins when transfected individually. (B) Localization of MDFIC with the indicated RELT family members when co-transfected together. (For interpretation of the references to color in this figure legend, the reader is referred to the Web version of this article.)

Fluor goat anti-rabbit IgG 555 and Alexa Fluor donkey anti-goat IgG 488 antibodies as secondary antibodies. All IF experiments included staining with DAPI.

Co-immunoprecipitation (Co-I) and western blotting. 293 cells (≈5 × 10^6) were transfected with 10 μg of the indicated expression plasmids and harvested as described previously [24]. Co-IP was performed using a kit from Sigma-Aldrich according to the manufacturer's instructions. For Co-IP of MDFIC with RELT, RELL1 or OSR1, 0.3 μg of either anti-Flag, anti-HA antibody, or IgG isotype control was utilized for the pull-downs, and western blots were performed using either an anti-Flag or anti-HA antibody. For Co-IP between MDFIC and RELL2, 5 μg of either anti-Flag, anti-HA, or IgG isotype control was utilized for the pull-downs, and western blots were performed using either an anti-Flag or an anti-HA antibody. A 30 μl lysate aliquot was saved before Co-IP for western analysis to verify protein expression. RELT deletion mutants were detected using a polyclonal anti-RELT antibody. IR-800 and IR-680 secondary antibodies were utilized for visualization of the western blots.

Computational analysis of the intrinsic disorder predisposition. The per-residue predisposition for intrinsic disorder of the proteins analyzed in this study human RELT (UniProt ID: Q969Z4); MDFIC p32 (UniProt ID: Q9P1T7); MDFIC p40 (UniProt ID: Q9P1T7-1); RELL1 (UniProt ID: Q8IUW5), and RELL2 (UniProt ID: Q8NC24) was evaluated by a set of predictors from the PONDR family, such as PONDR® VLXT, PONDR® VL3, PONDR® VSL2, and PONDR® FIT. Although PONDR® VLXT [25] is not the most accurate disorder predictor, this tool is known to have high sensitivity to local sequence peculiarities and can be used for identifying disorder-based interaction sites [26–28] PONDR® VSL2 is one of the more accurate stand-alone disorder predictors [29], and based on the comprehensive assessment of in silico predictors of intrinsic disorder, this tool was shown to perform reasonably well [30,31]. PONDR® VL3 possesses high accuracy in finding long IDPRs [32], whereas PONDR-FIT represents a metapredictor, which, being moderately more accurate than each of the component predictors, is one of the more accurate disorder predictors [33]. We also utilized an IUPred platform that was designed to recognize intrinsically disordered protein regions (IDPRs) from the amino acid sequence alone based on the estimated pairwise energy content and that predicts probability of a query protein to have short and long IDPRs [34–36]. We also evaluated the mean disorder propensity of target proteins which was calculated by averaging disorder profiles of individual predictors. Use of consensus for evaluation of intrinsic disorder is motivated by empirical observations that this approach usually increases the predictive performance compared to the use of a single predictor [31,37,38]. For the rapid generation of disorder profile plots for query proteins a DiSpi web crawler was used. In these analyses, the disorder scores above 0.5 are considered to correspond to disordered residues/regions, and disorder scores noticeably exceeding 0.1 are considered as flexible.

MobiDB-based intrinsic disorder analysis. The overall disorder status of human proteins RELT, MDFIC p32, MDFIC p40, RELL1, and RELL2 was further analyzed using the MobiDB database (http://mobidb.bio.unipd.it/) [39–41]. This platform represents outputs of ten intrinsic disorder predictors, such as two versions of DisEMBL [42], two versions of ESpritz [43], GlobPlot [44], JRONN [45], PONDR® VSL2B [29,46] and two versions of IUPred [34–36] and uses the outputs of these predictors to generate consensus disorder scores for query proteins. MobiDB also represents manually curated protein function and structure annotations derived from UniProt [47] and DisProt [48], as well as from Pfam [49] and PDB [50].

Prediction of disorder-based binding sites in the query proteins. Potential disorder-based binding sites in human RELT, MDFIC p32, MDFIC p40, RELL1, and RELL2 were predicted using the ANCHOR algorithm [51,52]. This approach relies on the pairwise energy estimation approach developed for the general disorder prediction method IUPred [34,35], being based on the hypothesis that long regions of disorder contain localized potential binding sites that cannot form enough favorable intrachain interactions to fold on their own, but are likely to gain stabilizing energy by interacting with a globular protein partner. This tool allows identification of molecular recognition features (MoRFs); i.e., specific functional elements, which are located within the longer IDPRs, are mostly disordered in their unbound states, and fold at interaction

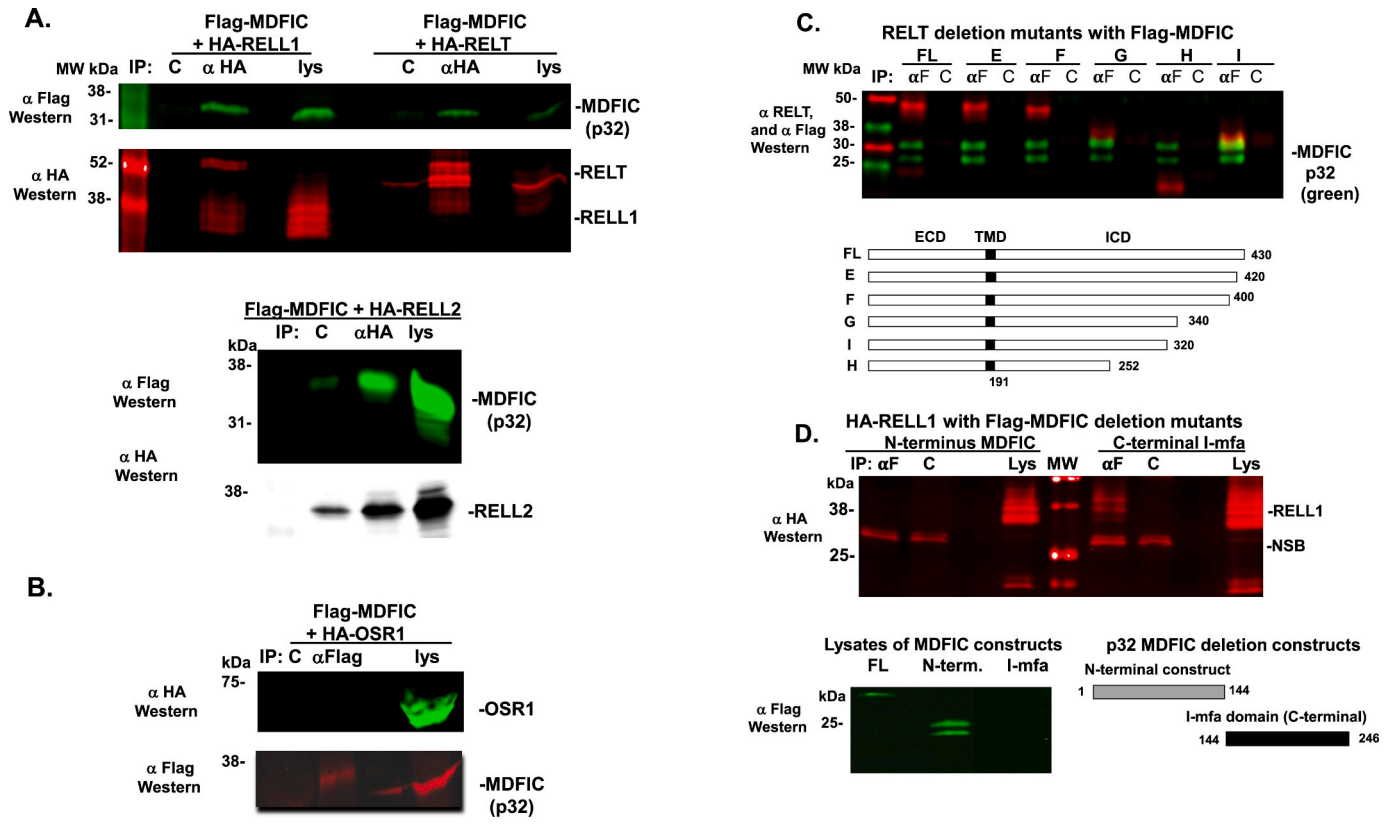

Fig. 3. MDFIC physically interacts with RELT family members. For all indicated experiments, 293 cells were transiently transfected with the indicated epitope-tagged expression plasmids for Co-immunoprecipitation (Co-IP) as described in Materials and Methods. A small amount of the protein lysate (lys) was saved to verify the expression of the epitope-tagged construct. Co-IP was performed using either an anti-HA (αHA), anti-Flag (αF) or IgG isotype control (C) antibody as the immunoprecipitating (IP) antibody. Western blot analysis was performed using either an anti-HA (αHA) or anti-Flag (αF) antibody as indicated. The size of molecular weight markers (MW) in kilodaltons (kDa) is indicated. (A). RELT family members physically interact with the p32 isoform of MDFIC. The expression plasmid for the Flag-tagged MDFIC was co-expressed with the indicated expression plasmids for HA-tagged RELT family members, and Co-IP was performed with an anti-HA antibody to pull-down the indicated RELT family member. (B). MDFIC does not physically interact with OSR1. An anti-Flag antibody was used to pull-down MDFIC as shown in the bottom panel (C). MDFIC physically interacts with regions of RELT proximal to the plasma membrane. The expression plasmid for MDFIC was co-transfected with expression plasmids for either full-length (FL) RELT, or deletion mutants for RELT, as indicated. An anti-Flag antibody was used to pull-down MFDIC. (D). RELL1 interacts with the I-mfa domain of MDFIC. The expression plasmid for RELL1 was co-transfected with expression plasmids for either the N-terminal fragment of the p32 isoform of MDFIC or the C-terminal I-mfa domain as indicated. An anti-Flag antibody was used to pull-down the indicated truncated versions of MDFIC. The positions of RELL1 and a non-specific band (NSB) observed in all Co-IP lanes are indicated. The expression of the N-terminal MDFIC construct and full-length (FL) construct in the protein lysates was confirmed as indicated.

with specific partners [27,28,53,54].

Functional disorder analysis. The D^2P^2 database (http://d2p2.pro/) [55] was used for the complementary evaluation of intrinsic disorder propensity of human RELT, MDFIC p32, MDFIC p40, RELL1, and RELL2. Some important disorder-related functional information was retrieved from this database too. D^2P^2 is a database of predicted disorder for a large library of proteins from completely sequenced genomes [55] that uses outputs of IUPred [34], PONDR® VLXT [25], PrDOS [56], PONDR® VSL2 [29], PV2 [55], and ESpritz [43]. The database is further supplemented by data concerning location of various functional domains, sites of curated posttranslational modifications, and predicted disorder-based protein binding sites. In addition, the D2P2 profile of a query protein contains information on the location of various posttranslational modifications and predicted disorder-based protein binding sites [55].

Immunohistochemistry (IHC). A total of 5 normal adult lymph nodes and 5 cases of B-cell lymphomas (2 low grade and 3 high grade) were examined; a total of 6 unstained sections for each of these 10 samples were utilized (therefore 60 slides combined). 20 of these slides were used for IF staining, IHC was performed as described previously [57] on the remaining 40 slides using a 1:100 overnight incubation with a RELT polyclonal antibody. A negative control was routinely performed in an identical fashion as the other samples with the exception that the primary RELT antibody was omitted. To estimate the intensity of immunostaining for RELT in the specimens, images were first inspected at low magnifications (4x and 10x) and the percentages of positively staining cells were evaluated. Each sample was next inspected at medium and medium-high magnifications (40x, 100x, respectively) to assign intensity values based on the semi-quantitative scale of 0–3, where 0 is no staining, 1 is weak, 2 is moderate and 3 is strong. Immunostaining intensity scores were calculated by using the following formula: weighted signal intensity = percentage of immunostained cells × average intensity score. A one-way ANOVA test was used to analyze the statistical significance between the different groups.

3. Results and discussion

A two-hybrid yeast genetic screen [58] was performed using the conserved intracellular domain (ICD) of RELL1 fused in-frame with the GAL4 DNA-binding domain as bait (Fig. 1). Approximately 1.2×10^6 and 1.0×10^6 clones from leukocyte and B-cell cDNA libraries were screened and the LIL18 clone was identified from the leukocyte library using the indicated RELL1 bait construct. DNA sequencing revealed LIL18 contains a portion of the *MDFIC* gene expressed in-frame with the GAL4 activation domain. MDFIC exists in two isoforms, p40 and p32,

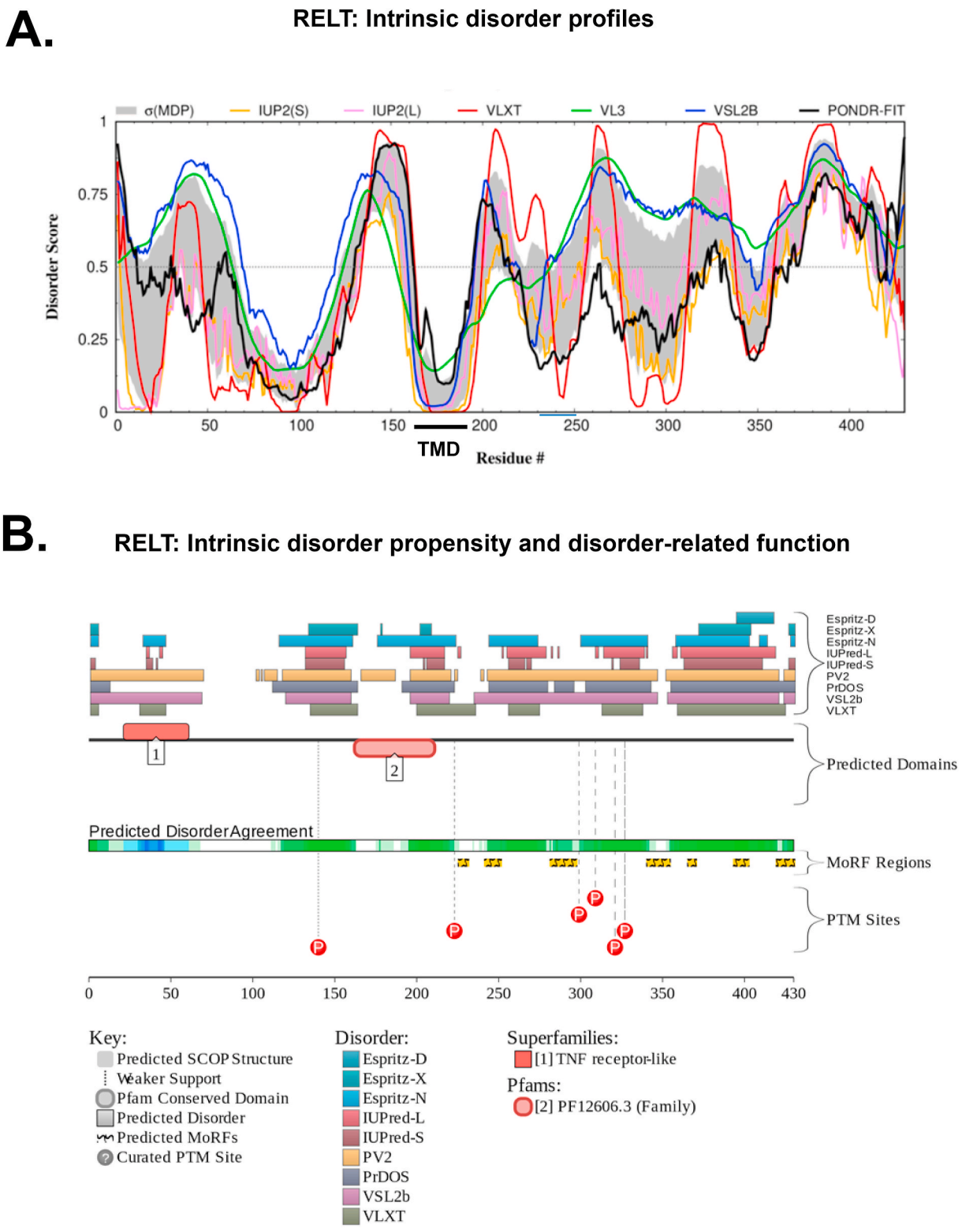

Fig. 4. Functional disorder analysis of human RELT and MDFIC p32. Intrinsic disorder profiles generated by DiSpi web-crawler for (A) RELT (UniProt ID: Q969Z4) and (C) MDFIC p32 (UniProt ID: Q9P1T7). Per-residue disorder predisposition was evaluated by PONDR® VLXT (red curves), PONDR® VL3 (green curves), PONDR® VSL2 (blue curves), PONDR® FIT (black curves), IUPred_Short (orange curves), and IUPred_Long (pink curves). Light gray shade shows distribution of standard deviations for the mean disorder predisposition. The transmembrane alpha helix (TMD) of RELT (163–183) and I-mfa domain of MDFIC p32 (144–246) are indicated. Intrinsic disorder propensity and some important disorder-related functional information generated for human RELT (B) and MDFIC p32 (D) by the D2P2 database (http://d2p2.pro/) [55]. Outputs of nine disorder predictors are shown by differently colored bars. The green-and-white bar in the middle of the plot shows the predicted disorder agreement between nine predictors, with green parts corresponding to disordered regions by consensus. Yellow bars show the locations of the predicted disorder-based binding sites (molecular recognition features, MoRFs), whereas colored circles at the bottom of the plots show location of phosphorylation (red) and acetylation (yellow) sites. (For interpretation of the references to color in this figure legend, the reader is referred to the Web version of this article.)

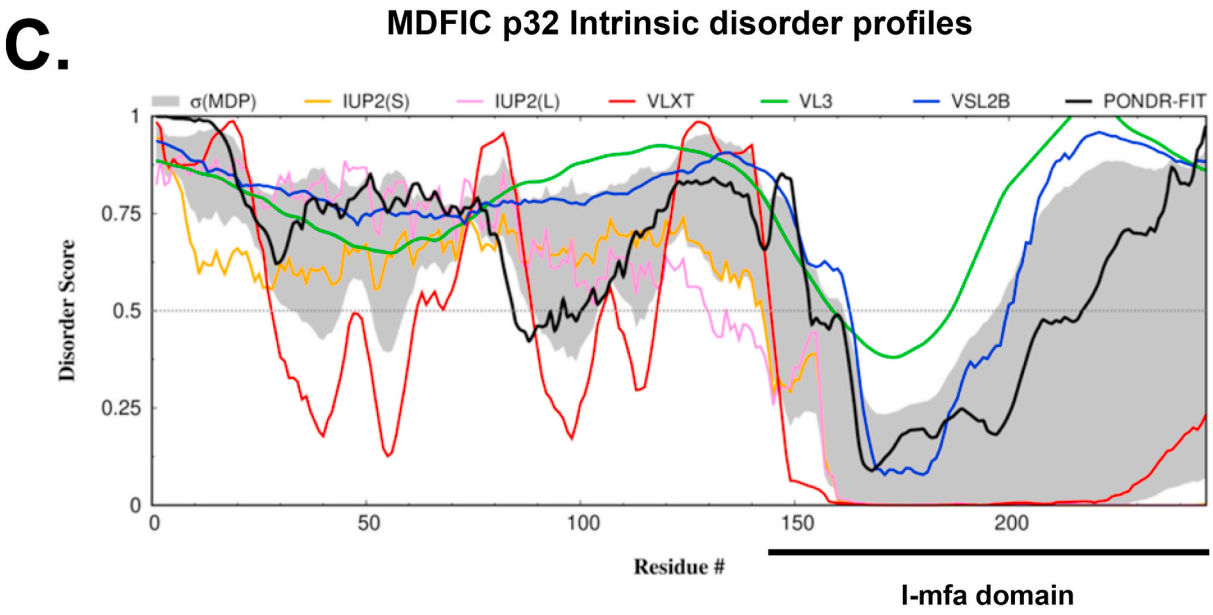

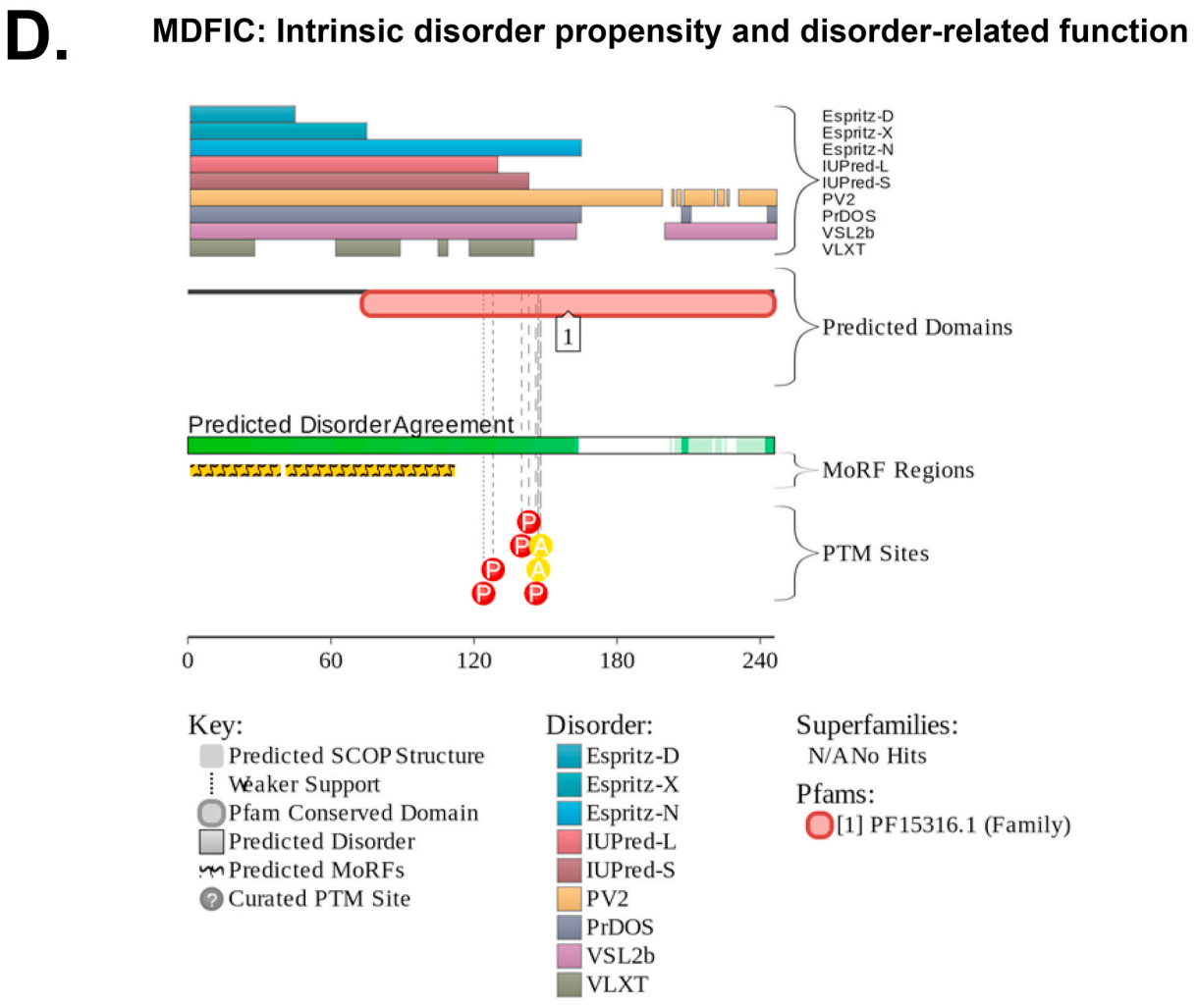

Fig. 4. (*continued*).

produced from differing translational start sites [23]. The LIL18 clone contained the entire coding sequence for p32 and a portion of amino-terminal sequences from p40 beginning at amino acid 82 and therefore contains one of the two basic regions of p40 implicated with nuclear import [23]. All experiments described in this report utilized p32, the most predominant isoform of MDFIC.

Immunofluorescence (IF) was utilized to observe the localization of MDFIC with RELT family members in 293 cells as described in Materials

and Methods. When expressed by itself, MDFIC was predominantly cytosolic (Fig. 2A), as has been reported previously [23,59]. RELL1 and RELL2 expressed individually were predominantly associated with the plasma membrane, whereas RELT displayed punctate cytosolic staining, consistent with previous observations [7,24]. Co-expression of MDFIC with either RELL1 or RELL2 resulted in prominent co-localization of the proteins at the plasma membrane. In contrast, the co-localization of MDFIC with RELT was not as consistently observed (Fig. 2B). However, the localization of some TNFRSF members is signal-dependent [60], and therefore it is conceivable that a more pronounced MDFIC-RELT co-localization could be dependent on an unidentified ligand, or other signaling molecules present in hematopoietic cells, but not in the 293s used in this study.

Co-immunoprecipitation (Co-IP) was used to confirm a physical interaction between MDFIC and RELT family members. HA-tagged RELT, RELL1, and RELL2 each pulled-down Flag-tagged MDFIC (Fig. 3A). Additionally, MDFIC pulled-down each of the HA-tagged RELT family members when the Co-IP was performed in the opposite direction (data not shown). MDFIC did not pull-down OSR1 in a Co-IP despite abundant expression of both proteins (Fig. 3B). MDFIC is not predicted to bind the kinase OSR1 due to the absence of the characteristic [S/G/V]RFx[V/I]xx[V/I/T/S]xx motif characteristic of OSR1-binding proteins [61]. The inability of MDFIC to pull down OSR1 indicates that the Co-IP conditions used to assess physical interactions between the epitope-tagged constructs were relatively specific.

Having confirmed a physical association between MDFIC and RELT family members, we next used deletion mutants in Co-IP experiments to identify regions that mediate these physical interactions. All five deletion mutants containing differing amounts of the RELT ICD [5] were successfully pulled down by MDFIC (Fig. 3C) and the electrophoretic migration of individual RELT mutants correlated with their expected sizes. p32 migrated as a doublet as has been described previously [62]. The carboxy-terminal I-mfa domain from MDFIC was capable of pulling down RELL1 in a Co-IP experiment (Fig. 3D). However, RELL1 was not pulled-down by the N-terminal domain of MDFIC, despite detectable expression in protein lysates (Fig. 3D). The Flag-tagged I-mfa domain was unexpectedly not detected by western blotting, despite the observed pull-down of RELL1, yet the inability to detect a Flag-tagged I-mfa domain by western blot has been reported previously [63]. Collectively, our results indicate that interactions between RELT family members and MDFIC occur between the I-mfa domain of MDFIC and regions of RELT family members proximal to the plasma membrane (amino acids 190–252 in RELT) which are devoid of conserved domains as indicated by using a traditional blast search.

We sought to determine the intrinsic predispositions for RELT and MDFIC due to both the inability to determine conserved motifs in the ICD of RELT family members, and due to reports in the literature indicating that both RELT and MDFIC are multifunctional proteins, which are often characterized by disordered structures. Results of this multifactorial analysis are summarized in Fig. 4. Fig. 4A and C shows disorder profiles generated for these proteins by DiSpi indicating their highly disordered status. In fact, the C-terminal half of RELT (residues 200–430) and the long N-terminal region of MFDIC p32 (residues 1–160) are predicted as mostly disordered. Overall, 45.6% and 60.2% of the human RELT and MFDIC residues are predicted to be disordered (have disorder scores above the 0.5 threshold) based on the averaging the outputs of the PONDR® VLXT, PONDR® VL3, PONDR® VSL2, PONDR® FIT, IUPred_short, and IUPred long predictors. This clearly places them into the category of highly disordered proteins, if the classification of proteins based on their percent of predicted disordered residues (PPIDR) values is used, where proteins are considered as highly ordered, moderately disordered, or highly disordered if their PPIDR$<$10%, 10%$\leq$ PPIDR$<$30%, or PPIDR$\geq$30%, respectively [64]. Even most stringent and conservative evaluation of the disorder content in human RELT and MFDIC (14.2% and 28.9%, respectively) by the MobiDB platform that aggregates the outputs from ten disorder predictors placed these two proteins into the category of moderately disordered proteins. Curiously, for a given query protein tools included into the MobiDB platform showed a broad variability of the disorder levels that ranges from 5.3% (ESpritz-DisProt) to 74.2% (PONDR® VSL2) in RELT and from 17.5% (ESpritz-DisProt) to 85% (PONDR® VSL2) in MFDIC.

Next, we analyzed prevalence of functional disorder in human RELT and MFDIC by the D^2P^2 platform (http://d2p2.pro/) [55], which in addition to the outputs of 9 disorder predictors shows predicted disorder agreement, presence of conserved functional domains, as well as location of predicted disorder-based protein binding sites and various posttranslational modifications (PTMs). Fig. 4B and D represent the D^2P^2 profiles of human RELT and MFDIC, provide further support to the highly disordered status of these proteins, and show that they contain multiple phosphorylation and acetylation sites, which are concentrated within the IDPRs of query proteins.

Multiple studies revealed that some IDPs/IDPRs are able to undergo at least partial disorder-to-order transitions upon binding, and such binding-induced folding is crucial for recognition, regulation, and signaling functions of these proteins [26–28,53,54,65–67]. Often, such disorder-based functional sites can be identified as short order-prone motifs located within the long IDPRs. Although such motifs do not have structure in their unbound forms, they are capable of the undergoing the binding-induced disorder-to-order transitions caused by their interaction with specific partners. Since these molecular recognition features (MoRFs) can be identified computationally [27], to find MoRFs in human RELT and MFDIC, we utilized a specialized algorithm, ANCHOR [51,52]. Fig. 4B and D includes the results of this analysis into the D^2P^2 profiles and shows that human RELT contains seven MoRFs, residues 225–231, 241–251, 281–297, 340–354, 365–370, 393–402 and 419–430, distributed within its C-terminal half, whereas one can find two MoRFs in human MFDIC p32 (residues 1–38 and 41–111). In other words, 18.1% and 60.6% residues of human RELT and MFDIC p32 can be potentially involved in disorder-based interactions, clearly indicating that intrinsic disorder in these proteins can be utilized in protein-protein interactions.

Therefore, results of previous studies clearly show that RELT and MFDIC are multifunctional proteins and our analysis indicates that RELT family members are intrinsically disordered proteins. Among various factors defining a capability of protein to be multifunctional is their remarkable structural heterogeneity defined by the predisposition for intrinsic disorder. In fact, a typical protein molecule is characterized by a complex mosaic structure, where different regions can be disordered to different degrees [68], and where a protein represents an assembly of foldons (independent foldable units of a protein), inducible foldons (disordered regions that can fold at least in part due to the interaction with binding partners), non-foldons (non-foldable protein regions), semi-foldons (regions that are always in a semi-folded form), and unfoldons (ordered regions that have to undergo an order-to-disorder transition to become functional) [68–70]. Obviously, such structural mosaic defines the capability of a protein to have a multitude of unrelated functions and be involved in interaction with a host of structurally unrelated partners, with the resulting structural and functional heterogeneity of proteins serving as a foundation of the structure-function continuum concept [71–73].

The discovery that MDFIC interacts with RELT family members is a novel finding deserving of further exploration given that RELT and MDFIC share many similarities. MDFIC and RELT are both highly expressed in tissues and cells of the hematopoietic system [4,5,23] and both proteins exhibit high levels of expression in resting T cells that subsequently drops upon T-cell activation [6,74]. Initial attempts to identify the physiological relevance of RELT and p32 interactions were inconclusive and are worthy of further exploration. Although this study focused on the p32, the LIL18 clone obtained in this study contained part of the p40 isoform, and therefore, it is possible that RELT family members also interact with p40 isoform.

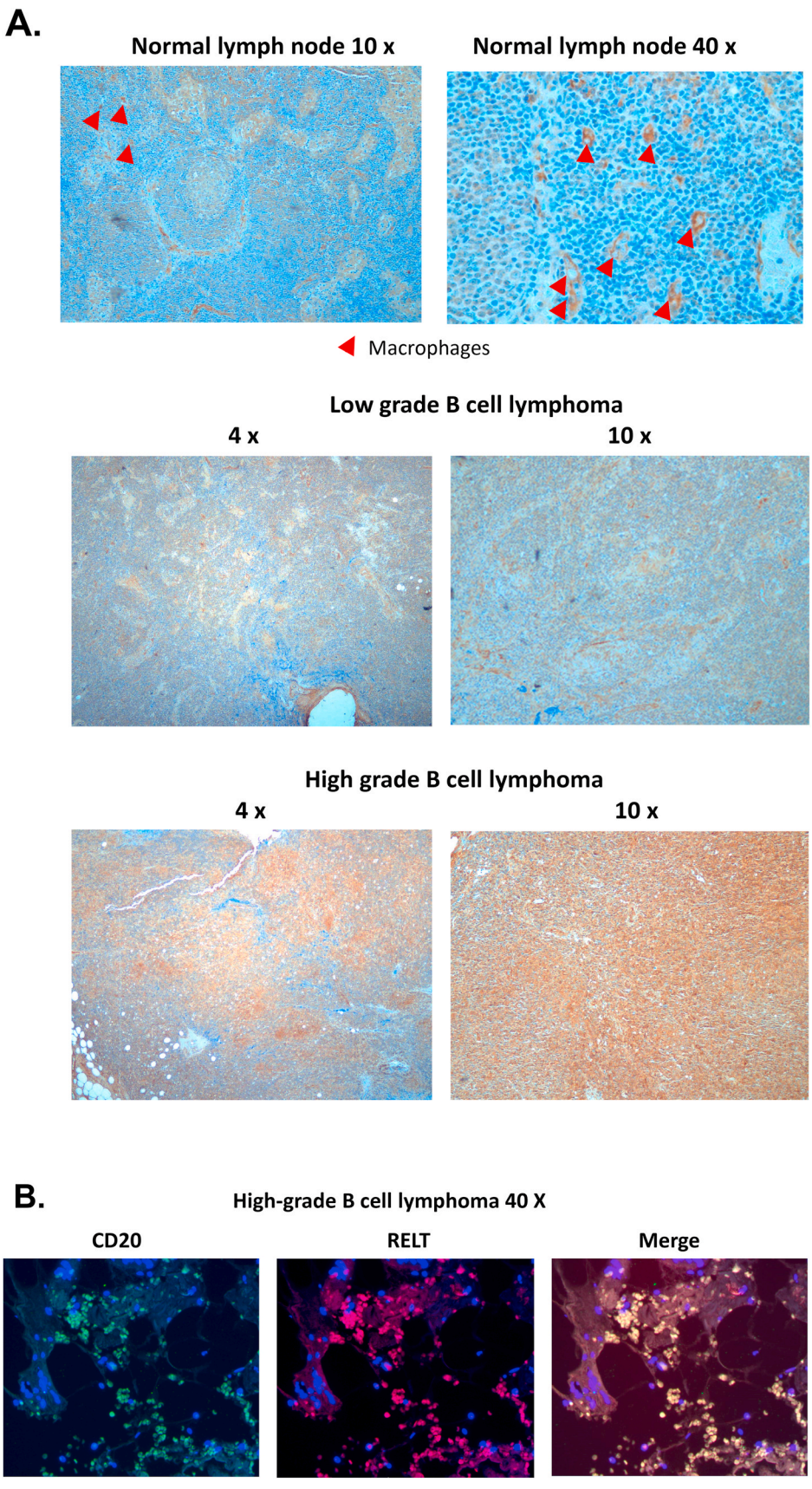

Fig. 5. RELT is expressed in human lymph nodes and B-cell lymphomas. Immunohistochemistry was performed on both normal lymph nodes and resected B-cell lymphomas using an antibody directed against RELT as described in Materials and Methods. (A) Comparison of RELT staining in normal lymph nodes, low-grade, and high-grade B-cell lymphomas. RELT staining at the indicated magnification with the presence of macrophages in normal lymph nodes indicated by red arrowheads. (B) RELT co-localizes with CD20 in B-cell lymphomas. Immunofluorescence was conducted with RELT and CD20 antibodies as described in Materials and Methods resulting in RELT fluorescing red, CD20 fluorescing green, and DAPI staining nuclei blue. Photographs were taken at 40x magnification. (For interpretation of the references to color in this figure legend, the reader is referred to the Web version of this article.)

Table 1
Statistical analysis of protein levels of RELT in clinical lymph node specimens.

Sample	RELT staining intensity Mean (±SEM N = 8)
Normal Lymph Node	53.8 ± 19.3
Low-Grade B-cell Lymphoma	81.3 ± 18.2
High-Grade B-cell Lymphoma	185 ± 34.6

RELT protein expression was semi-quantitatively measured in clinical lymph node specimens. The data are presented as the mean ± standard error of the mean. A one-way ANOVA test used to analyze the staining revealed that the staining differences between the three groups was statistically significant ($p < 0.05$).

Multiple lines of evidence suggest that MDFIC regulates transcription, and both p32 and p40 isoforms are capable of modulating transcription by sequestering transcription factors in the cytosol and nucleolus respectively [75]. MDFIC has additional capabilities to influence transcription besides sequestration, as MDFIC influences global transcriptional events by altering the phosphorylation status of the glucocorticoid receptor [62]. MDFIC also influences signal transduction pathways including the Wnt/β-catenin and JNK pathways [76,77]. MDFIC is epigenetically silenced in cancerous hematopoietic cell lines, suggesting it may function as a tumor suppressor [78], an idea supported by the observation that ectopic expression of MDFIC suppresses the growth of a colorectal cancer cell line [79]. Yet the impact of MDFIC on cancer cells may be cancer cell-specific, as MDFIC expression enhanced the chemoresistance of cancer stem cells in a lung cancer cell model [80].

Since RELT is prominently expressed in the hematopoietic system, we sought to characterize the expression of RELT in lymphoid organs. Immunohistochemistry (IHC) was utilized to detect the presence of RELT in normal human lymph nodes as well as B-cell lymphomas. RELT staining was consistently observed in normal lymph nodes and the staining appeared strongest in macrophages (Fig. 5A). RELT staining was also observed in additional areas of lymph nodes such as in germinal centers and endothelial cells. The staining was dependent on the presence of the RELT primary antibody as indicated by the negative control (data not shown). RELT staining in high-grade B-cell lymphomas was of higher intensity than either normal lymph nodes or low-grade B-cell lymphomas and this increase was statistically significant (Table 1). IF was utilized to determine whether RELT was expressed in the infiltrating B cells of B-cell lymphomas. Co-localization of RELT and CD20 in the smaller lymphocytes was observed and was particularly evident in the high-grade B-cell lymphoma sections (Fig. 5B). Collectively, this report identifies and characterizes interactions between MDFIC and RELT family members and provides preliminary evidence that RELT expression is associated with the cancerous infiltrating B lymphocytes of B-cell lymphomas. This report therefore expands our limited knowledge of the evolutionarily conserved RELT family members.

CRediT authorship contribution statement

John K. Cusick: Conceptualization, Investigation, Resources, Writing - original draft, Visualization, Supervision. **Yasmeen Alhomsy:** Investigation. **Stephanie Wong:** Investigation. **George Talbott:** Investigation, Supervision. **Vladimir N. Uversky:** Formal analysis, Investigation, Visualization, Writing - original draft. **Cara Hart:** Investigation. **Nazila Hejazi:** Supervision, Formal analysis. **Aaron T. Jacobs:** Investigation, Resources, Writing - review & editing. **Yihui Shi:** Formal analysis, Investigation, Writing - review & editing.

Declaration of competing interest

The authors declare that they have no known competing financial interests or personal relationships that could have appeared to influence the work reported in this paper.

Acknowledgments

Slides of normal and malignant human lymph node tissue provided by the UC Davis Comprehensive Cancer Center, supported by grant NCI P30CA093373. The authors wish to thank Pachai Moua, Dino Aghains, Leo Fitzpatrick, and Dhammika Atapattu for their contributions to this manuscript. This work was supported in part by Grant #T32 AI000048 to John Kappler. Additional funding was provided by California Northstate University (Elk Grove, CA), California University of Science and Medicine (San Bernardino, CA), and the University of Hawaii at Hilo (Hilo, HI).

References

[1] B.B. Aggarwal, S.C. Gupta, J.H. Kim, Historical perspectives on tumor necrosis factor and its superfamily: 25 years later, a golden journey, Blood 119 (2012) 651–665, https://doi.org/10.1182/blood-2011-04-325225.
[2] T. Hehlgans, K. Pfeffer, The intriguing biology of the tumour necrosis factor/tumour necrosis factor receptor superfamily: players, rules and the games, Immunology 115 (2005) 1–20, https://doi.org/10.1111/j.1365-2567.2005.02143.x.
[3] M. Croft, C.A. Benedict, C.F. Ware, Clinical targeting of the TNF and TNFR superfamilies, Nat Rev Drug Discov 12 (2013) 147–168, https://doi.org/10.1038/nrd3930.
[4] G.L. Sica, G. Zhu, K. Tamada, D. Liu, J. Ni, L. Chen, RELT, a new member of the tumor necrosis factor receptor superfamily, is selectively expressed in hematopoietic tissues and activates transcription factor NF-kappaB, Blood 97 (2001) 2702–2707, https://doi.org/10.1182/blood.v97.9.2702.
[5] P. Moua, M. Checketts, L.G. Xu, H.B. Shu, M.E. Reyland, J.K. Cusick, RELT family members activate p38 and induce apoptosis by a mechanism distinct from TNFR1, Biochem Biophys Res Commun 491 (2017) 25–32, https://doi.org/10.1016/j.bbrc.2017.07.022.
[6] B.K. Choi, S.H. Kim, Y.H. Kim, D.G. Lee, H.S. Oh, C. Han, Y.I. Kim, Y. Jeon, H. Lee, B.S. Kwon, RELT negatively regulates the early phase of the T-cell response in mice, Eur J Immunol 48 (2018) 1739–1749, https://doi.org/10.1002/eji.201847633.
[7] J.K. Cusick, L.G. Xu, L.H. Bin, K.J. Han, H.B. Shu, Identification of RELT homologues that associate with RELT and are phosphorylated by OSR1, Biochem Biophys Res Commun 340 (2006) 535–543, https://doi.org/10.1016/j.bbrc.2005.12.033.
[8] J.K. Cusick, A. Mustian, K. Goldberg, M.E. Reyland, RELT induces cellular death in HEK 293 epithelial cells, Cell Immunol 261 (2010) 1–8, https://doi.org/10.1016/j.cellimm.2009.10.013.
[9] T.C. Polek, M. Talpaz, T. Spivak-Kroizman, The TNF receptor, RELT, binds SPAK and uses it to mediate p38 and JNK activation, Biochem Biophys Res Commun 343 (2006) 125–134, https://doi.org/10.1016/j.bbrc.2006.02.125.
[10] D. Wu, P. Zhang, J. Ma, J. Xu, L. Yang, W. Xu, H. Que, M. Chen, H. Xu, Serum biomarker panels for the diagnosis of gastric cancer, Cancer Med 8 (2019) 1576–1583, https://doi.org/10.1002/cam4.2055.
[11] L. Zhong, K. Ge, J.C. Zu, L.H. Zhao, W.K. Shen, J.F. Wang, X.G. Zhang, X. Gao, W. Hu, Y. Yen, K.H. Kernstine, Autoantibodies as potential biomarkers for breast cancer, Breast Cancer Res 10 (2008) R40, https://doi.org/10.1186/bcr2091.
[12] H. Jung, S. Park, G.R. Gunassekaran, M. Jeon, Y.E. Cho, M.C. Baek, J.Y. Park, G. Shim, Y.K. Oh, I.S. Kim, C. Kim, B. Lee, A peptide probe enables photoacoustic-guided imaging and drug delivery to lung tumors in K-ras(LA2) mutant mice, Cancer Res 79 (2019) 4271–4282, https://doi.org/10.1158/0008-5472.CAN-18-3089.
[13] A. Ikeda, S. Shahid, B.R. Blumberg, M. Suzuki, J.D. Bartlett, ADAM10 is expressed by ameloblasts, cleaves the RELT TNF receptor extracellular domain and facilitates enamel development, Sci Rep 9 (2019) 14086, https://doi.org/10.1038/s41598-019-50277-y.
[14] J.W. Kim, H. Zhang, F. Seymen, M. Koruyucu, Y. Hu, J. Kang, Y.J. Kim, A. Ikeda, Y. Kasimoglu, M. Bayram, C. Zhang, K. Kawasaki, J.D. Bartlett, T.L. Saunders, J. P. Simmer, J.C. Hu, Mutations in RELT cause autosomal recessive amelogenesis imperfecta, Clin Genet 95 (2019) 375–383, https://doi.org/10.1111/cge.13487.
[15] G. Nikolopoulos, C.E.L. Smith, S.J. Brookes, M.E. El-Asrag, C.J. Brown, A. Patel, G. Murillo, M.J. O'Connell, C.F. Inglehearn, A.J. Mighell, New missense variants in RELT causing hypomineralised amelogenesis imperfecta, Clin Genet 97 (2020) 688–695, https://doi.org/10.1111/cge.13721.
[16] L. Feng, J. Hu, W. Zhang, Y. Dong, S. Xiong, C. Dong, RELL1 inhibits autophagy pathway and regulates Mycobacterium tuberculosis survival in macrophages, Tuberculosis (Edinb) 120 (2020) 101900, https://doi.org/10.1016/j.tube.2020.101900.
[17] Y. Li, W. Shang, G. Xiao, L.K. Zhang, C. Zheng, A comparative quantitative proteomic analysis of HCMV-infected cells highlights pUL138 as a multifunctional protein, Molecules 25 (2020), https://doi.org/10.3390/molecules25112520.
[18] X. Jin, H. Xie, X. Liu, Q. Shen, Z. Wang, H. Hao, Y. Gu, RELL1, a novel oncogene, accelerates tumor progression and regulates immune infiltrates in glioma, Int Immunopharmacol 87 (2020) 106707, https://doi.org/10.1016/j.intimp.2020.106707.

[19] P. Wang, Q. Yang, X. Du, Y. Chen, T. Zhang, Targeted regulation of Rell2 by microRNA-18a is implicated in the anti-metastatic effect of polyphyllin VI in breast cancer cells, Eur J Pharmacol 851 (2019) 161–173, https://doi.org/10.1016/j.ejphar.2019.02.041.
[20] S.J. Tang, H. Shen, O. An, H. Hong, J. Li, Y. Song, J. Han, D.J.T. Tay, V.H.E. Ng, F. Bellido Molias, K.W. Leong, P. Pitcheshwar, H. Yang, L. Chen, Cis- and trans-regulations of pre-mRNA splicing by RNA editing enzymes influence cancer development, Nat Commun 11 (2020) 799, https://doi.org/10.1038/s41467-020-14621-5.
[21] H.S. Huang, X.Y. Huang, H.Z. Yu, Y. Xue, P.L. Zhu, Circular RNA circ-RELL1 regulates inflammatory response by miR-6873-3p/MyD88/NF-kappaB axis in endothelial cells, Biochem Biophys Res Commun 525 (2020) 512–519, https://doi.org/10.1016/j.bbrc.2020.02.109.
[22] G. Angenard, A. Merdrignac, C. Louis, J. Edeline, C. Coulouarn, Expression of long non-coding RNA ANRIL predicts a poor prognosis in intrahepatic cholangiocarcinoma, Dig Liver Dis 51 (2019) 1337–1343, https://doi.org/10.1016/j.dld.2019.03.019.
[23] S. Thebault, F. Gachon, I. Lemasson, C. Devaux, J.M. Mesnard, Molecular cloning of a novel human I-mfa domain-containing protein that differently regulates human T-cell leukemia virus type I and HIV-1 expression, J Biol Chem 275 (2000) 4848–4857, https://doi.org/10.1074/jbc.275.7.4848.
[24] J.K. Cusick, A. Mustian, A.T. Jacobs, M.E. Reyland, Identification of PLSCR1 as a protein that interacts with RELT family members, Mol Cell Biochem 362 (2012) 55–63, https://doi.org/10.1007/s11010-011-1127-4.
[25] P. Romero, Z. Obradovic, X. Li, E.C. Garner, C.J. Brown, A.K. Dunker, Sequence complexity of disordered protein, Proteins 42 (2001) 38–48, https://doi.org/10.1002/1097-0134(20010101)42:1<38::aid-prot50>3.0.co.
[26] A.K. Dunker, J.D. Lawson, C.J. Brown, R.M. Williams, P. Romero, J.S. Oh, C. J. Oldfield, A.M. Campen, C.M. Ratliff, K.W. Hipps, J. Ausio, M.S. Nissen, R. Reeves, C. Kang, C.R. Kissinger, R.W. Bailey, M.D. Griswold, W. Chiu, E. C. Garner, Z. Obradovic, Intrinsically disordered protein, J Mol Graph Model 19 (2001) 26–59, https://doi.org/10.1016/s1093-3263(00)00138-8.
[27] C.J. Oldfield, Y. Cheng, M.S. Cortese, P. Romero, V.N. Uversky, A.K. Dunker, Coupled folding and binding with alpha-helix-forming molecular recognition elements, Biochemistry 44 (2005) 12454–12470, https://doi.org/10.1021/bi050736e.
[28] Y. Cheng, C.J. Oldfield, J. Meng, P. Romero, V.N. Uversky, A.K. Dunker, Mining alpha-helix-forming molecular recognition features with cross species sequence alignments, Biochemistry 46 (2007) 13468–13477, https://doi.org/10.1021/bi7012273.
[29] Z. Obradovic, K. Peng, S. Vucetic, P. Radivojac, A.K. Dunker, Exploiting heterogeneous sequence properties improves prediction of protein disorder, Proteins 61 (Suppl 7) (2005) 176–182, https://doi.org/10.1002/prot.20735.
[30] Z.L. Peng, L. Kurgan, Comprehensive comparative assessment of in-silico predictors of disordered regions, Curr Protein Pept Sci 13 (2012) 6–18, https://doi.org/10.2174/138920312799277938.
[31] X. Fan, L. Kurgan, Accurate prediction of disorder in protein chains with a comprehensive and empirically designed consensus, J Biomol Struct Dyn 32 (2014) 448–464, https://doi.org/10.1080/07391102.2013.775969.
[32] Z. Obradovic, K. Peng, S. Vucetic, P. Radivojac, C.J. Brown, A.K. Dunker, Predicting intrinsic disorder from amino acid sequence, Proteins 53 (Suppl 6) (2003) 566–572, https://doi.org/10.1002/prot.10532.
[33] B. Xue, R.L. Dunbrack, R.W. Williams, A.K. Dunker, V.N. Uversky, PONDR-FIT: a meta-predictor of intrinsically disordered amino acids, Biochim Biophys Acta 1804 (2010) 996–1010, https://doi.org/10.1016/j.bbapap.2010.01.011.
[34] Z. Dosztanyi, V. Csizmok, P. Tompa, I. Simon, IUPred: web server for the prediction of intrinsically unstructured regions of proteins based on estimated energy content, Bioinformatics 21 (2005) 3433–3434, https://doi.org/10.1093/bioinformatics/bti541.
[35] Z. Dosztanyi, V. Csizmok, P. Tompa, I. Simon, The pairwise energy content estimated from amino acid composition discriminates between folded and intrinsically unstructured proteins, J Mol Biol 347 (2005) 827–839, https://doi.org/10.1016/j.jmb.2005.01.071.
[36] B. Meszaros, G. Erdos, Z. Dosztanyi, IUPred2A: context-dependent prediction of protein disorder as a function of redox state and protein binding, Nucleic Acids Res 46 (2018) W329–W337, https://doi.org/10.1093/nar/gky384.
[37] I. Walsh, M. Giollo, T. Di Domenico, C. Ferrari, O. Zimmermann, S.C. Tosatto, Comprehensive large-scale assessment of intrinsic protein disorder, Bioinformatics 31 (2015) 201–208, https://doi.org/10.1093/bioinformatics/btu625.
[38] Z. Peng, L. Kurgan, On the complementarity of the consensus-based disorder prediction, Pac Symp Biocomput (2012) 176–187.
[39] T. Di Domenico, I. Walsh, A.J. Martin, S.C. Tosatto, MobiDB: a comprehensive database of intrinsic protein disorder annotations, Bioinformatics 28 (2012) 2080–2081, https://doi.org/10.1093/bioinformatics/bts327.
[40] M. Necci, D. Piovesan, Z. Dosztanyi, S.C.E. Tosatto, MobiDB-lite: fast and highly specific consensus prediction of intrinsic disorder in proteins, Bioinformatics 33 (2017) 1402–1404, https://doi.org/10.1093/bioinformatics/btx015.
[41] D. Piovesan, F. Tabaro, L. Paladin, M. Necci, I. Micetic, C. Camilloni, N. Davey, Z. Dosztanyi, B. Meszaros, A.M. Monzon, G. Parisi, E. Schad, P. Sormanni, P. Tompa, M. Vendruscolo, W.F. Vranken, S.C.E. Tosatto, MobiDB 3.0: more annotations for intrinsic disorder, conformational diversity and interactions in proteins, Nucleic Acids Res 46 (2018) D471–D476, https://doi.org/10.1093/nar/gkx1071.
[42] R. Linding, L.J. Jensen, F. Diella, P. Bork, T.J. Gibson, R.B. Russell, Protein disorder prediction: implications for structural proteomics, Structure 11 (2003) 1453–1459, https://doi.org/10.1016/j.str.2003.10.002.
[43] I. Walsh, A.J. Martin, T. Di Domenico, S.C. Tosatto, ESpritz: accurate and fast prediction of protein disorder, Bioinformatics 28 (2012) 503–509, https://doi.org/10.1093/bioinformatics/btr682.
[44] R. Linding, R.B. Russell, V. Neduva, T.J. Gibson, GlobPlot, Exploring protein sequences for globularity and disorder, Nucleic Acids Res 31 (2003) 3701–3708, https://doi.org/10.1093/nar/gkg519.
[45] Z.R. Yang, R. Thomson, P. McNeil, R.M. Esnouf, RONN: the bio-basis function neural network technique applied to the detection of natively disordered regions in proteins, Bioinformatics 21 (2005) 3369–3376, https://doi.org/10.1093/bioinformatics/bti534.
[46] K. Peng, S. Vucetic, P. Radivojac, C.J. Brown, A.K. Dunker, Z. Obradovic, Optimizing long intrinsic disorder predictors with protein evolutionary information, J Bioinform Comput Biol 3 (2005) 35–60, https://doi.org/10.1142/s0219720005000886.
[47] R. Apweiler, A. Bairoch, C.H. Wu, W.C. Barker, B. Boeckmann, S. Ferro, E. Gasteiger, H. Huang, R. Lopez, M. Magrane, M.J. Martin, D.A. Natale, C. O'Donovan, N. Redaschi, L.S. Yeh, UniProt: the universal protein knowledgebase, Nucleic Acids Res 32 (2004) D115–D119, https://doi.org/10.1093/nar/gkh131.
[48] M. Sickmeier, J.A. Hamilton, T. LeGall, V. Vacic, M.S. Cortese, A. Tantos, B. Szabo, P. Tompa, J. Chen, V.N. Uversky, Z. Obradovic, A.K. Dunker, DisProt: the database of disordered proteins, Nucleic Acids Res 35 (2007) D786–D793, https://doi.org/10.1093/nar/gkl893.
[49] R.D. Finn, A. Bateman, J. Clements, P. Coggill, R.Y. Eberhardt, S.R. Eddy, A. Heger, K. Hetherington, L. Holm, J. Mistry, E.L. Sonnhammer, J. Tate, M. Punta, Pfam: the protein families database, Nucleic Acids Res 42 (2014) D222–D230, https://doi.org/10.1093/nar/gkt1223.
[50] H.M. Berman, J. Westbrook, Z. Feng, G. Gilliland, T.N. Bhat, H. Weissig, I. N. Shindyalov, P.E. Bourne, The protein data bank, Nucleic Acids Res 28 (2000) 235–242, https://doi.org/10.1093/nar/28.1.235.
[51] B. Meszaros, I. Simon, Z. Dosztanyi, Prediction of protein binding regions in disordered proteins, PLoS Comput Biol 5 (2009), e1000376, https://doi.org/10.1371/journal.pcbi.1000376.
[52] Z. Dosztanyi, B. Meszaros, I. Simon, ANCHOR: web server for predicting protein binding regions in disordered proteins, Bioinformatics 25 (2009) 2745–2746, https://doi.org/10.1093/bioinformatics/btp518.
[53] A. Mohan, C.J. Oldfield, P. Radivojac, V. Vacic, M.S. Cortese, A.K. Dunker, V. N. Uversky, Analysis of molecular recognition features (MoRFs), J Mol Biol 362 (2006) 1043–1059, https://doi.org/10.1016/j.jmb.2006.07.087.
[54] V. Vacic, C.J. Oldfield, A. Mohan, P. Radivojac, M.S. Cortese, V.N. Uversky, A. K. Dunker, Characterization of molecular recognition features, MoRFs, and their binding partners, J Proteome Res 6 (2007) 2351–2366, https://doi.org/10.1021/pr0701411.
[55] M.E. Oates, P. Romero, T. Ishida, M. Ghalwash, M.J. Mizianty, B. Xue, Z. Dosztanyi, V.N. Uversky, Z. Obradovic, L. Kurgan, A.K. Dunker, J. Gough, D(2)P(2): database of disordered protein predictions, Nucleic Acids Res 41 (2013) D508–D516, https://doi.org/10.1093/nar/gks1226.
[56] T. Ishida, K. Kinoshita, PrDOS: prediction of disordered protein regions from amino acid sequence, Nucleic Acids Res 35 (2007) W460–W464, https://doi.org/10.1093/nar/gkm363.
[57] L.W. Maines, L.R. Fitzpatrick, K.J. French, Y. Zhuang, Z. Xia, S.N. Keller, J. J. Upson, C.D. Smith, Suppression of ulcerative colitis in mice by orally available inhibitors of sphingosine kinase, Dig Dis Sci 53 (2008) 997–1012, https://doi.org/10.1007/s10620-007-0133-6.
[58] S. Fields, R. Sternglanz, The two-hybrid system: an assay for protein-protein interactions, Trends Genet 10 (1994) 286–292, https://doi.org/10.1016/0168-9525(90)90012-u.
[59] S. Thebault, J. Basbous, B. Gay, C. Devaux, J.M. Mesnard, Sequence requirement for the nucleolar localization of human I-mfa domain-containing protein (HIC p40), Eur J Cell Biol 79 (2000) 834–838, https://doi.org/10.1078/0171-9335-00111.
[60] S.J. Jones, E.C. Ledgerwood, J.B. Prins, J. Galbraith, D.R. Johnson, J.S. Pober, J. R. Bradley, TNF recruits TRADD to the plasma membrane but not the trans-Golgi network, the principal subcellular location of TNF-R1, J Immunol 162 (1999) 1042–1048.
[61] E. Delpire, K.B. Gagnon, Genome-wide analysis of SPAK/OSR1 binding motifs, Physiol Genomics 28 (2007) 223–231, https://doi.org/10.1152/physiolgenomics.00173.2006.
[62] R.H. Oakley, J.M. Busillo, J.A. Cidlowski, Cross-talk between the glucocorticoid receptor and MyoD family inhibitor domain-containing protein provides a new mechanism for generating tissue-specific responses to glucocorticoids, J Biol Chem 292 (2017) 5825–5844, https://doi.org/10.1074/jbc.M116.758888.
[63] V.W. Gautier, N. Sheehy, M. Duffy, K. Hashimoto, W.W. Hall, Direct interaction of the human I-mfa domain-containing protein, HIC, with HIV-1 Tat results in cytoplasmic sequestration and control of Tat activity, Proc Natl Acad Sci U S A 102 (2005) 16362–16367, https://doi.org/10.1073/pnas.0503519102.
[64] K. Rajagopalan, S.M. Mooney, N. Parekh, R.H. Getzenberg, P. Kulkarni, A majority of the cancer/testis antigens are intrinsically disordered proteins, J Cell Biochem 112 (2011) 3256–3267, https://doi.org/10.1002/jcb.23252.
[65] H.J. Dyson, P.E. Wright, Coupling of folding and binding for unstructured proteins, Curr Opin Struct Biol 12 (2002) 54–60, https://doi.org/10.1016/s0959-440x(02)00289-0.
[66] H.J. Dyson, P.E. Wright, Intrinsically unstructured proteins and their functions, Nat Rev Mol Cell Biol 6 (2005) 197–208, https://doi.org/10.1038/nrm1589.

[67] V.N. Uversky, Intrinsic disorder-based protein interactions and their modulators, Curr Pharm Des 19 (2013) 4191–4213, https://doi.org/10.2174/1381612811319230005.
[68] V.N. Uversky, Unusual biophysics of intrinsically disordered proteins, Biochim Biophys Acta 1834 (2013) 932–951, https://doi.org/10.1016/j.bbapap.2012.12.008.
[69] V.N. Uversky, A.K. Dunker, The case for intrinsically disordered proteins playing contributory roles in molecular recognition without a stable 3D structure, F1000, Biol Rep 5 (2013) 1, https://doi.org/10.3410/B5-1.
[70] V.N. Uversky, A decade and a half of protein intrinsic disorder: biology still waits for physics, Protein Sci 22 (2013) 693–724, https://doi.org/10.1002/pro.2261.
[71] V.N. Uversky, p53 proteoforms and intrinsic disorder: an illustration of the protein structure-function continuum concept, Int J Mol Sci 17 (2016), https://doi.org/10.3390/ijms17111874.
[72] V.N. Uversky, Functional roles of transiently and intrinsically disordered regions within proteins, FEBS J 282 (2015) 1182–1189, https://doi.org/10.1111/febs.13202.
[73] V.N. Uversky, Protein intrinsic disorder and structure-function continuum, Prog Mol Biol Transl Sci 166 (2019) 1–17, https://doi.org/10.1016/bs.pmbts.2019.05.003.
[74] S. Kusano, M. Yoshimitsu, M. Hachiman, M. Ikeda, I-mfa domain proteins specifically interact with HTLV-1 Tax and repress its transactivating functions, Virology 486 (2015) 219–227, https://doi.org/10.1016/j.virol.2015.09.020.
[75] S. Thebault, J.M. Mesnard, How the sequestration of a protein interferes with its mechanism of action: example of a new family of proteins characterized by a particular cysteine-rich carboxy-terminal domain involved in gene expression regulation, Curr Protein Pept Sci 2 (2001) 155–167, https://doi.org/10.2174/1389203013381143.
[76] S. Kusano, Y. Eizuru, Human I-mfa domain proteins specifically interact with KSHV LANA and affect its regulation of Wnt signaling-dependent transcription, Biochem Biophys Res Commun 396 (2010) 608–613, https://doi.org/10.1016/j.bbrc.2010.04.111.
[77] S. Kusano, N. Raab-Traub, I-mfa domain proteins interact with Axin and affect its regulation of the Wnt and c-Jun N-terminal kinase signaling pathways, Mol Cell Biol 22 (2002) 6393–6405, https://doi.org/10.1128/mcb.22.18.6393-6405.2002.
[78] L. Gu, J. Dean, A.L. Oliveira, N. Sheehy, W.W. Hall, V.W. Gautier, Expression profile and differential regulation of the Human I-mfa domain-Containing protein (HIC) gene in immune cells, Immunol Lett 123 (2009) 179–184, https://doi.org/10.1016/j.imlet.2009.03.010.
[79] Y. Sui, X. Li, S. Oh, B. Zhang, W.M. Freeman, S. Shin, R. Janknecht, Opposite roles of the JMJD1A interaction partners MDFI and MDFIC in colorectal cancer, Sci Rep 10 (2020) 8710, https://doi.org/10.1038/s41598-020-65536-6.
[80] C.J. Chen, C.J. Yang, S.F. Yang, M.S. Huang, Y.P. Liu, The MyoD family inhibitor domain-containing protein enhances the chemoresistance of cancer stem cells in the epithelial state by increasing beta-catenin activity, Oncogene 39 (2020) 2377–2390, https://doi.org/10.1038/s41388-019-1152-4.